Trinuclear and Tetranuclear Platinum−Iridium Cluster Complexes: A Remarkable Metal for Metal Substitution Reaction

Brian T. Sterenberg,† Greg J. Spivak,† Glenn P. A. Yap,‡ and Richard J. Puddephatt*,†

Department of Chemistry, University of Western Ontario, London, Ontario, Canada N6A 5B7, and Department of Chemistry and Biochemistry, University of Windsor, Windsor, Ontario, Canada N9B 3P4

Received February 12, 1998

The reaction of $[Pt_3(\mu_3\text{-}CO)(\mu\text{-}dppm)_3]^{2+}$, **1**, dppm = $Ph_2PCH_2PPh_2$, with $[Ir(CO)_4]^-$ at low temperature gives $[Pt_3(\mu_3\text{-}CO)(\mu\text{-}dppm)_3\{Ir(CO)_4\}]^+$, **2**, and subsequent loss of CO leads to the butterfly complex $[Pt_3\{Ir(CO)(\mu\text{-}CO)_2\}(\mu\text{-}CO)(\mu\text{-}dppm)_3]^+$, **3**. Complex **3** reacts with L = $P(OPh)_3$ to give $[Pt_3\{IrL(\mu\text{-}CO)_2\}(\mu\text{-}CO)(\mu\text{-}dppm)_3]^+$, **4**, which has been characterized by X-ray structure determination and has a butterfly structure with iridium at a wingtip position. Cluster **3** is thermally unstable and rearranges in solution to form the isomeric butterfly cluster cation $[Pt_2Ir\{Pt(CO)(\mu\text{-}CO)_2\}(CO)(\mu\text{-}dppm)_3]^+$, **5**, in which the iridium atom now occupies a hinge position and whose formation involves phosphorus migration from platinum to iridium. Under CO, **5** eliminates one platinum atom to form the trimetallic complex $[Pt_2Ir(\mu_3\text{-}CO)(CO)(\mu\text{-}dppm)_3]^+$, **6**. The overall reaction then involves displacement of a platinum atom from the 42-electron cluster cation **1** by $\{IrCO\}^-$ to give the 44-electron cation **6**.

Introduction

There is currently interest in modeling bimetallic catalysts, such as Pt−Ir, Pt−Re and Pt−Sn on alumina, which are important in petroleum refining, by well-characterized heteronuclear cluster complexes.[1] Platinum−iridium−alumina catalysts are normally sulfided before use and have advantages over simple platinum−alumina catalysts in maintaining activity for longer periods and in having higher selectivity for dehydrocyclization of linear alkanes.[2] There are relatively few known platinum−iridium cluster complexes;[1b] the crystallographically characterized examples include $[Pt_2Ir_2(\mu\text{-}CO)_3(CO)_4(PPh_3)_3]$, $[Ir_3Pt_3(\mu\text{-}CO)_3(CO)_3(\eta^5\text{-}C_5Me_5)_3]$, and $[PtIr_4(CO)_9(\mu\text{-}CO)_n]^{2-}$ (n = 3 or 5)[3] and a number of examples stabilized with bridging ligands;[4] some of these are illustrated in Chart 1.

This paper reports a number of Pt_3Ir and Pt_2Ir clusters which are formed by reaction of a triplatinum cluster $[Pt_3(\mu_3\text{-}CO)(\mu\text{-}dppm)_3]^{2+}$ with the nucleophilic reagent $[Ir(CO)_4]^-$. The reaction leads to an overall metal atom substitution by a stepwise addition, rearrangement, dissociation sequence. It should be noted that the formation of mixed-metal clusters by such addition−dissociation sequences is already well-established,[5−7] but the present system has unique features. The metal addition step has been observed previously in the formation of a tetrahedral PtRe cluster by reaction of $[Pt_3(\mu_3\text{-}CO)(\mu\text{-}dppm)_3]^{2+}$ with $[Re(CO)_5]^-$.[8] A preliminary account of part of this work has been published.[9]

Chart 1

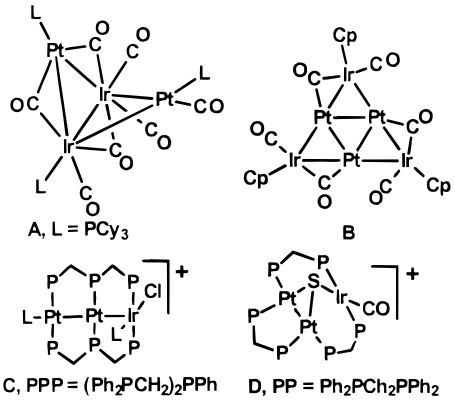

† University of Western Ontario.
‡ University of Windsor.

(1) (a) Guczi, L. *Metal Clusters in Catalysis*; Gates, B. C., Guczi, L., Knozinger, H., Eds.; Elsevier: New York, 1986. (b) Farrugia, L. J. *Adv. Organomet. Chem.* **1990**, *31*, 301. (c) Adams, R. D.; Hermann, W. A. *Polyhedron* **1988**, *7*, 2255. (d) Sinfelt, J. H. *Bimetallic Catalysts: Discoveries, Concepts and Applications*; Wiley: New York, 1983. (e) Xiao, J.; Puddephatt, R. J. *Coord. Chem. Rev.* **1995**, *143*, 457.

(2) (a) Rasser, J. C.; Beindorff, W. H.; Scholten, J. J. F. *J. Catal.* **1979**, *59*, 211. (b) Rice, R. W.; Lu, K. *J. Catal.* **1982**, *77*, 104. (c) Yang, O. B.; Woo, S. I.; Ryoo, R. *J. Catal.* **1992**, *137*, 357.

(3) (a) Bhaduri, S.; Sharma, K. R.; Clegg, W.; Sheldrick, G. M.; Stalke, D. *J. Chem. Soc., Dalton Trans.* **1984**, 2851. (b) Freeman, M. J.; Miles, A. D.; Murray, M.; Orpen, A. G.; Stone, F. G. A. *Polyhedron* **1984**, *3*, 1093. (c) Fumagalli, A.; Pergola, R. D.; Bonacina, F.; Garlaschelli, L.; Moret, M.; Sironi, A. *J. Am. Chem. Soc.* **1989**, *111*, 165.

(4) (a) Stang, P. J.; Huang, Y. H.; Arif, A. M. *Organometallics* **1992**, *11*, 845. (b) Balch, A. L.; Catalano, V. J. *Inorg. Chem.* **1992**, *31*, 2569. (c) Hadj-Bagheri, N.; Puddephatt, R. J. *Inorg. Chim. Acta* **1993**, *213*, 29. (d) Tanase, T.; Toda, H.; Kobayashi, K.; Yamamoto, Y. *Organometallics* **1996**, *15*, 5272.

(5) Vahrenkamp, H. *Adv. Organomet. Chem.* **1983**, *22*, 169.

(6) Adams, R. D.; Babin, J. E.; Miklos, T. *Organometallics* **1988**, *7*, 219.

(7) Mingos, D. M. P.; May, A. S. *The Chemistry of Metal Cluster Complexes*; Shriver, D. F., Adams, R. D., Eds.; VCH: New York, 1990.

(8) Xiao, J.; Kristof, E.; Vittal, J. J.; Puddephatt, R. J. *J. Organomet. Chem.* **1995**, *490*, 1.

S0276-7333(98)00095-8 CCC: $15.00
Publication on Web 05/13/1998

Scheme 1

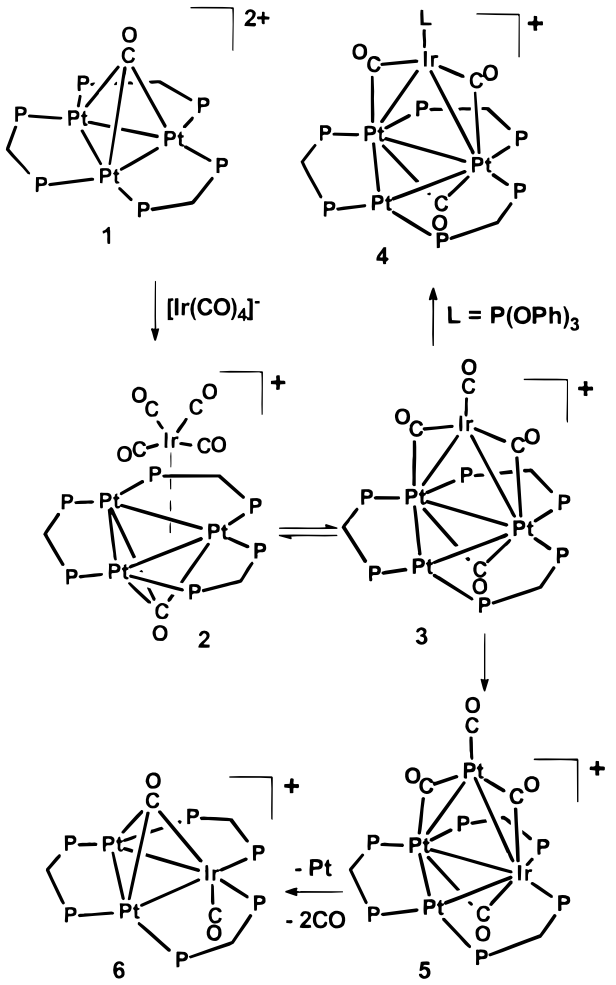

Results and Discussion

A summary of the new chemistry is shown in Scheme 1, and the synthesis and characterization of the Pt/Ir clusters is described below.

Synthesis of Pt_3Ir Butterfly Clusters. By analogy with the known reaction of $[Pt_3(\mu_3\text{-}CO)(\mu\text{-}dppm)_3]^{2+}$, **1**, with $[Re(CO)_5]^-$ to give the tetrahedral 54-electron Pt_3Re cluster $[Pt_3\{\mu_3\text{-}Re(CO)_3\}(\mu\text{-}dppm)_3]^+$,[8] it was considered that the reaction of **1** with $[Ir(CO)_4]^-$ might give a tetrahedral Pt_3Ir cluster cation. However, the reaction resulted instead in the rapid formation of the dark red 58-electron cluster $[Pt_3\{Ir(CO)(\mu\text{-}CO)_2\}(\mu\text{-}CO)(\mu\text{-}dppm)_3][PF_6]$, **3**, which has an unusual butterfly structure with the iridium occupying a wingtip position (Scheme 1). Complex **3** in solution decomposes slowly at room temperature as described below and so cannot easily be purified; it was characterized spectroscopically and by conversion to the more stable derivative **4**. Thus, the terminal carbonyl ligand in **3** was readily replaced by reaction with $L = P(OPh)_3$ to give the phosphite derivative $[Pt_3\{IrL(\mu\text{-}CO)_2\}(\mu\text{-}CO)(\mu\text{-}dppm)_3][PF_6]$, **4**.

Complexes **3** and **4** have been characterized spectroscopically, and **4** has been structurally characterized by X-ray diffraction. A view of the structure of the cation is given in Figure 1. Selected bond distances and angles are shown in Table 1, and crystal data are given in

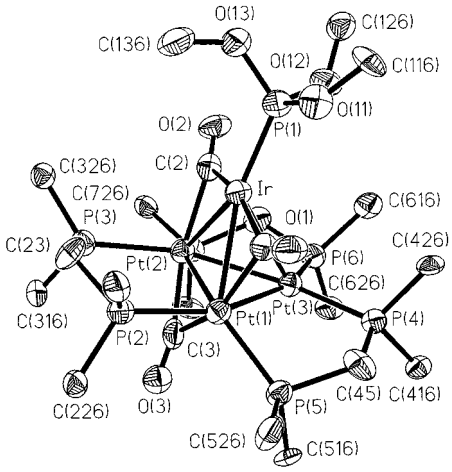

Figure 1. View of the structure of the cation $[Pt_3\{Ir(\mu\text{-}CO)_2(P(OPh)_3)\}(\mu\text{-}CO)(\mu\text{-}dppm)_3]^+$, **4**. Thermal ellipoids are drawn at 30% probability, and only the *ipso* carbon atoms of the phenyl groups are shown for clarity. Note the near planarity of the P(1)IrPt(1)Pt(2)(μ-CO)$_3$ unit.

Table 2. The Pt_3Ir core of **4** has a butterfly structure with iridium at one of the wingtip positions. Thus, the Pt(3)−Ir distance of 3.002(1) Å is considerably longer than the other Pt−Ir or Pt−Pt distances (2.634(1)−2.727(1) Å) and is best considered a nonbonding distance. The hinge angle Ir−Pt(1)−Pt(2)−Pt(3) of 70.5° is typical of butterfly clusters.[1,3a,10] Each edge of the Pt_3 triangle is bridged by a dppm ligand, while each edge of the Pt(1)Pt(2)Ir triangle is bridged by a carbonyl ligand. The atoms of the P(1)IrPt(1)Pt(2)(μ-CO)$_3$ unit are approximately coplanar. The carbonyl-bridged metal−metal distances (Pt(1)−Pt(2) = 2.711(1) Å, Pt(1)−Ir = 2.679(1) Å, Pt(2)−Ir = 2.727(1) Å) are longer than the unbridged ones (Pt(1)−Pt(3) = 2.634(1) Å, Pt(2)−Pt(3) = 2.649(1) Å),[3] and the carbonyls bridging the Pt−Ir bonds are essentially symmetrical (Ir−C(1) = 2.00(2) Å, Pt(1)−C(1) = 2.17(2) Å, Ir−C(2) = 2.10(2) Å, Pt(2)−C(2) = 2.06(2) Å; Ir−C(1)−O(1) = 145(2)°; Pt(1)−C(1)−O(1) = 135(2)°, Ir−C(2)−O(2) = 134(2)°, Pt(2)−C(2)−O(2) = 144(2)°).

The IR spectra of **3** and **4** each contain three bands due to the μ-CO ligands in the range 1890−1765 cm^{-1}, and **3** also has a terminal carbonyl band with ν(CO) = 1982 cm^{-1}. The similarity of the IR and ^{31}P NMR (vide infra) data for **3** and **4** is a clear indication that they have the same structure. However, the NMR data at room temperature suggest that the molecules have 3-fold symmetry. For example, each gives a single ^{31}P resonance for the dppm phosphorus atoms in the ^{31}P NMR spectra, and this is not consistent with the solid-state structure (Figure 1) found for **4**. The apparent problem is readily rationalized in terms of fluxionality, as discussed below. The ^{13}C NMR spectrum (Figure 2) of a ^{13}CO-labeled sample of **3** shows three resonances at δ 188.8 (terminal CO, L^a in Chart 2) and 214.8 and 239.7 (bridging CO, C^b and C^c in Chart 2). The terminal carbonyl resonance appears as a 1:4:7:4:1 multiplet due to coupling to platinum-195 with ^2J(PtC^a) = 43 Hz, indicating a long-range coupling to three equivalent Pt

(9) Spivak, G. J.; Yap, G. P. A.; Puddephatt, R. J. *Polyhedron* **1997**, *16*, 3861.

(10) Douglas, G.; Manojlovic-Muir, Lj.; Muir, K. W.; Jennings, M. C.; Lloyd, N. R.; Rashidi, M.; Schoettel, G.; Puddephatt, R. J. *Organometallics* **1991**, *10*, 3927.

Table 1. Selected Bond Lengths (Å) and Angles (deg) for $[Pt_3\{Ir(\mu\text{-}CO)_2(P(OPh)_3)\}(\mu\text{-}Co)(\mu\text{-}dppm)_3][PF_6]$, 4

Ir−C(1)	2.00(2)	Pt(1)−Pt(2)	2.711(1)
Ir−C(2)	2.10(2)	Pt(2)−C(3)	1.96(2)
Ir−P(1)	2.183(5)	Pt(2)−C(2)	2.06(2)
Ir−Pt(1)	2.679(1)	Pt(2)−P(7)	2.298(5)
Ir−Pt(2)	2.727(1)	Pt(2)−P(3)	2.346(5)
Ir−Pt(3)	3.002(1)	Pt(2)−Pt(3)	2.6491(9)
Pt(1)−C(1)	2.17(2)	Pt(3)−P(6)	2.253(5)
Pt(1)−P(5)	2.281(4)	Pt(3)−P(4)	2.275(4)
Pt(1)−P(2)	2.332(5)	O(1)−C(1)	1.14(2)
Pt(1)−C(3)	2.29(2)	O(2)−C(2)	1.16(2)
Pt(1)−Pt(3)	2.634(1)	O(3)−C(3)	1.18(2)
C(1)−Ir−C(2)	160.9(8)	C(1)−Ir−Pt(3)	84.9(6)
C(1)−Ir-P(1)	101.4(6)	C(2)−Ir−Pt(3)	79.6(5)
C(2)−Ir−P(1)	96.9(6)	P(1)−Ir−Pt(3)	128.6(1)
C(1)−Ir−Pt(1)	52.7(6)	Pt(1)−Ir−Pt(3)	54.90(2)
C(2)−Ir−Pt(1)	108.6(5)	Pt(2)−Ir−Pt(3)	54.83(2)
P(1)−Ir−Pt(1)	154.1(1)	C(1)−Pt(1)−P(5)	93.8(6)
C(1)−Ir−Pt(2)	112.9(6)	C(1)−Pt(1)−P(2)	95.1(5)
C(2)−Ir−Pt(2)	48.5(5)	P(5)−Pt(1)−P(2)	112.9(2)
P(1)−Ir−Pt(2)	145.5(1)	C(1)−Pt(1)−C(3)	153.1(8)
Pt(1)−Ir−Pt(2)	60.19(3)	P(5)−Pt(1)−C(3)	108.1(6)
P(2)−Pt(1)−C(3)	90.6(5)	C(2)−Pt(2)−Pt(3)	89.3(5)
C(1)−Pt(1)−Pt(3)	91.6(5)	P(7)−Pt(2)−Pt(3)	92.3(1)
P(5)−Pt(1)−Pt(3)	90.1(1)	P(3)−Pt(2)−Pt(3)	154.1(1)
P(2)−Pt(1)−Pt(3)	155.4(1)	C(3)−Pt(2)−Pt(1)	55.9(7)
C(3)−Pt(1)−Pt(3)	73.4(5)	C(2)−Pt(2)−Pt(1)	108.5(5)
C(1)−Pt(1)−Ir	47.3(6)	P(7)−Pt(2)−Pt(1)	143.5(1)
P(5)−Pt(1)−Ir	132.3(1)	P(3)−Pt(2)−Pt(1)	95.3(1)
P(2)−Pt(1)−Ir	99.0(1)	Pt(3)−Pt(2)−Pt(1)	58.87(2)
C(3)−Pt(1)−Ir	105.9(6)	C(3)−Pt(2)−Ir	114.9(7)
Pt(3)−Pt(1)−Ir	68.81(3)	C(2)−Pt(2)−Ir	49.6(5)
C(1)−Pt(1)−Pt(2)	108.1(6)	P(7)−Pt(2)−Ir	134.2(1)
P(5)−Pt(1)−Pt(2)	142.0(1)	P(3)−Pt(2)−Ir	100.9(1)
P(2)−Pt(1)−Pt(2)	96.1(1)	Pt(3)−Pt(2)−Ir	67.89(3)
C(3)−Pt(1)−Pt(2)	45.1(6)	Pt(1)−Pt(2)−Ir	59.02(3)
Pt(3)−Pt(1)−Pt(2)	59.40(2)	P(6)−Pt(3)−P(4)	107.3(2)
Ir−Pt(1)−Pt(2)	60.79(3)	P(6)−Pt(3)−Pt(1)	157.2(1)
C(3)−Pt(2)−C(2)	163.6(8)	P(4)−Pt(3)−Pt(1)	95.2(1)
C(3)−Pt(2)−P(7)	99.5(7)	P(6)−Pt(3)−Pt(2)	95.9(1)
C(2)−Pt(2)−P(7)	91.5(5)	P(4)−Pt(3)−Pt(2)	156.6(1)
C(3)−Pt(2)−P(3)	86.5(5)	Pt(1)−Pt(3)−Pt(2)	61.73(3)
C(2)−Pt(2)−P(3)	101.0(5)	P(6)−Pt(3)−Ir	117.1(1)
P(7)−Pt(2)−P(3)	110.9(2)	P(4)−Pt(3)−Ir	107.8(1)
C(3)−Pt(2)−Pt(3)	78.2(5)	Pt(1)−Pt(3)−Ir	56.29(2)
Pt(2)−Pt(3)−Ir	57.29(2)	O(2)−C(2)−Ir	134(2)
O(1)−C(1)−Ir	145(2)	Pt(2)−C(2)−Ir	81.9(8)
O(1)−C(1)−Pt(1)	135(2)	O(3)−C(3)−Pt(2)	155(2)
Ir−C(1)−Pt(1)	80.0(9)	O(3)−C(3)−Pt(1)	126(2)
O(2)−C(2)−Pt(2)	144(2)	Pt(2)−C(3)−Pt(1)	79.0(8)

atoms,[11] while the chemical shift is in the range expected for terminally bound carbonyls. The long-range Pt coupling is consistent with this carbonyl occupying a terminal position on Ir approximately trans to the Ir−Pt bonds; fluxionality accounts for the apparent equivalence of the three platinum atoms. The resonance at δ 214.8 again appears as a 1:4:7:4:1 multiplet with $^1J(PtC^b) = 310$ Hz and is assigned as the carbonyl on the opposite face of the Pt_3 unit from the iridium. The resonance at $\delta(C^c)$ 239.7 is assigned to the two equivalent carbonyls which bridge between Ir and Pt. Although no ^{195}Pt coupling is observed, the chemical shift clearly indicates that the carbonyls bridge.

The observation of a butterfly structure is not unexpected since **3** and **4** have 58-electron configurations as in $[Pt_2Ir_2(\mu\text{-}CO)_3(CO)_4L_3]$ (**A**, Chart 1)[3a] and several homonuclear Pt_4 clusters.[10] Such clusters are electron precise, and the wingtip and hinge atoms have 16- and 18-electron configurations, respectively. Since iridium has a greater tendency to adopt an 18-electron configuration, it is expected to have a preference for the hinge position, and this is what is found in cluster **A**.[3a] Indeed, in all known electron-precise Pt−Ir carbonyl clusters, namely in **A**, the raft cluster $[Pt_3Ir_3(C_5Me_5)_3(CO)_3(\mu\text{-}CO)_3]$, and $[PtIr_2(indenyl)_2(CO)_3(PCy_3)]$, the platinum and iridium atoms have 16- and 18-electron configurations, respectively.[3] It is, therefore, remarkable that in **3** and **4** the iridium atom is in a wingtip position with a 16-electron configuration, and the rearrangement of **3** (vide infra) demonstrates the instability of this configuration. The reason for this unusual situation is clearly the presence of the relatively inert $Pt_3(\mu\text{-}dppm)_3$ unit, which does not allow a structure with two platinum atoms in wingtip positions without dissociation of Pt−P bonds. Note that electron counting for **3**, supported by EHMO calculations for the model cluster $[Pt_3Ir(\mu\text{-}CO)_3(CO)(\mu\text{-}H_2PCH_2PH_2)_3]^+$, requires a negative charge on iridium and positive charges on the two platinum atoms in the hinge positions. The com-

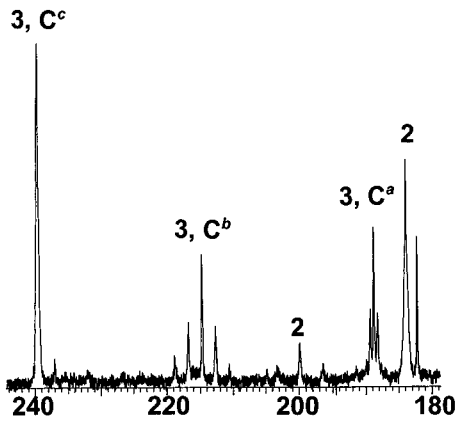

Figure 2. ^{13}C NMR spectrum (75 MHz) of an equilibrium mixture of $[Pt_3\{Ir(CO)_4\}(\mu_3\text{-}CO)(\mu\text{-}dppm)_3][PF_6]$, **2**, and $[Pt_3\{Ir(CO)(\mu\text{-}CO)_2\}(\mu\text{-}CO)(\mu\text{-}dppm)_3][PF_6]$, **3**, at −50 °C. The sharp singlet at δ 182 is due to free $[Ir(CO)_4]^-$, and the broader resonance at δ 184 is due to coordinated $[Ir(CO)_4]^-$ in **2**.

Table 2. Crystal Data and Structure Refinement for $[Pt_3\{Ir(\mu\text{-}CO)_2(P(OPh)_3)\}(\mu\text{-}Co)(\mu\text{-}dppm)_3][PF_6]$, 4

empirical formula	$C_{96}H_{81}F_6IrO_6P_8Pt_3$
fw	2469.84
temp	298(2) K
wavelength	0.71073 Å
cryst system	monoclinic
space group	$P2_1/c$
unit cell dimens	$a = 15.016(1)$ Å $b = 34.618(2)$ Å $c = 19.615(1)$ Å $\beta = 106.662(1)°$
vol., Z	9768.5(11) Å^3, 4
density (calcd)	1.679 Mg/m^3
abs coeff	5.833 mm^{-1}
$F(000)$	4760
cryst size	0.20 × 0.10 × 0.10 mm
Θ range data collection	1.42−22.50°
limiting indices	$-17 \le h \le 17$, $-19 \le k \le 41$, $-23 \le l \le 23$
no. of reflns collected	34 655
no. of indep reflns	12 713 [R(int) = 0.0646]
refinement method	full-matrix least-squares on F^2
data/restraints/params	12581/81/866
goodness-of-fit on F^2	0.986
R indices[$I > 2\sigma(I)$]	R1 = 0.0680, wR2 = 0.1747
R indices (all data)	R1 = 0.1182, wR2 = 0.2219
largest diff peak/hole	3.098/−1.714 e Å^{-3}

(11) Xiao, J.; Hao, L.; Puddephatt, R. J.; Manojlovic-Muir, Lj.; Muir, K. W.; Torabi, A. A. *Organometallics* **1995**, *14*, 4183.

Chart 2

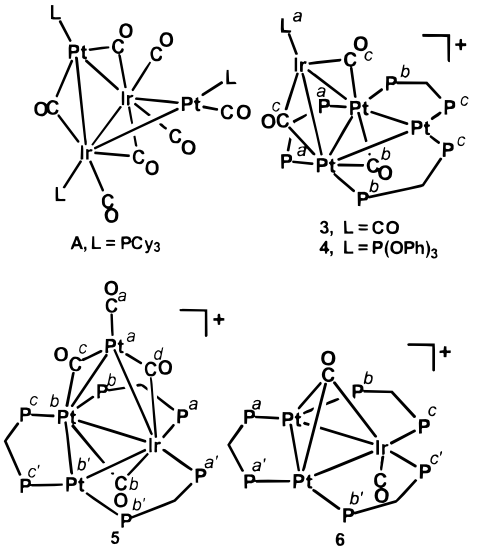

puted charges on the $Ir(CO)(\mu\text{-}CO)_2$ and $[Pt_3(\mu\text{-}CO)(\mu\text{-}H_2PCH_2PH_2)_3]$ fragments were −1.5 and +2.5 e, respectively. If formation of **3** is considered to occur by combination of $[Ir(CO)_3]^-$ and $[Pt_3(\mu\text{-}CO)(\mu\text{-dppm})_3]^{2+}$ fragments, little net electron transfer occurs.

The clusters **3** and **4** are highly fluxional. At ambient temperature, the ^{31}P NMR spectrum of **3** shows a sharp singlet for the phosphorus atoms of the μ-dppm ligands, with the complex pattern of Pt satellites that is typical of $Pt_3(\mu\text{-dppm})_3$ complexes with C_3 symmetry ($^1J(PtP) = 3132$ Hz). At −90 °C, the apparent C_3 symmetry is broken and the ^{31}P resonance separates into three very broad resonances (δ −1.5, −11.5, and −21.5), attributed to the nonequivalent phosphorus atoms P^a, P^b, and P^c (Chart 2). Similarly, the dppm resonance in the ^{31}P NMR spectrum of **4** at ambient temperature appears as a sharp doublet due to long-range coupling to the phosphite phosphorus atom ($^3J_{PP} = 16$ Hz, $^1J_{PtP} = 3242$ Hz). In agreement, the phosphite resonance appears as a septet, indicating the effective equivalence of the six dppm phosphorus atoms, and also gave a 1:4:7:4:1 multiplet ($^2J(PtP) = 508$ Hz), indicating coupling to three equivalent Pt atoms. At −90 °C, the dppm resonance splits into three very broad resonances (δ −7, −9, and −19) while the $P(OPh)_3$ resonance is also very broad. The spectra indicate that the $Ir(\mu\text{-}CO)_2L$ unit can migrate very easily about one side of the Pt_3 face, with the $Pt_2(\mu\text{-}C^bO)$ ligand migrating about the other side, leading to effective 3-fold symmetry (Scheme 2). The observation of the long-range coupling $^3J(Pt-P(OPh)_3)$ under the condition of fast fluxionality clearly eliminates the alternative mechanism involving reversible dissociation of the $[Ir(CO)_2L]^-$ unit from the cluster.

An Intermediate Cluster Cation $[Pt_3\{Ir(CO)_4\}(\mu_3\text{-}CO)(\mu\text{-dppm})_3]^+$, 2. When samples of **3** were prepared in situ in a sealed NMR tube, the low-temperature ^{31}P NMR spectrum revealed the presence of a second compound **2**. Further studies showed that this complex **2** is in equilibrium with **3** and is favored at lower temperatures and at higher CO pressure. These data indicate that **2** is a carbonyl adduct of **3**. If the initial reaction of $[Pt_3(\mu_3\text{-}CO)(dppm)_3][PF_6]_2$ with $[PPN][Ir(CO)_4]$ is carried out at −80 °C and the NMR spectrum is acquired at −80 °C without warming the

Scheme 2

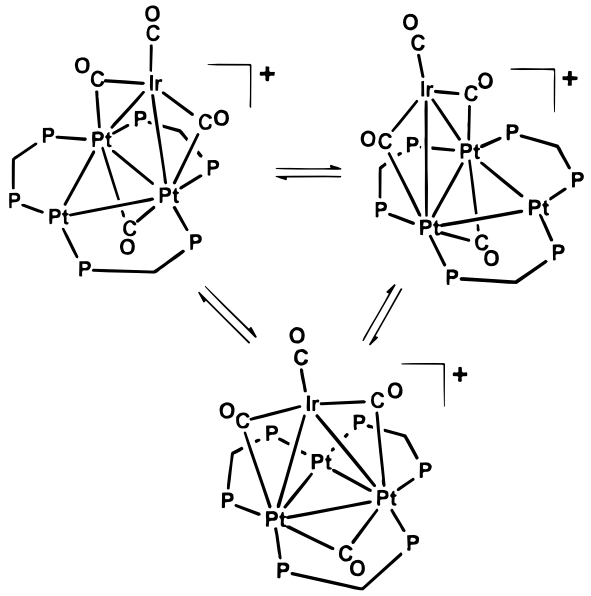

sample, no CO evolution is observed and essentially pure samples of **2** can be formed, thus indicating that the stoichiometry of the product **2** must be $[Pt_3(CO)(dppm)_3\{Ir(CO)_4\}]^+$. The ^{31}P NMR spectrum of **2** shows a singlet at δ −22.4, which shows the complex Pt satellites typical of $Pt_3(\mu\text{-dppm})_3$ complexes having effective C_3 symmetry, and, in this case, the spectrum remains sharp to −90 °C. The ^{13}C NMR spectrum of **2** shows two carbonyl resonances at δ 183.7 and 199.5 in a ratio of 4:1 (Figure 2). The first resonance appears as a broad singlet and is assigned to terminal carbonyls on iridium, based on the chemical shift (note the similarity to free $[Ir(CO)_4]^-$ in Figure 2) and the absence of Pt coupling. The second resonance is a 1:4:7:4:1 multiplet ($^1J(PtC) = 503$ Hz) similar to that of μ_3-carbonyl in **1** ($\delta = 205$, $^1J(PtC) = 777$ Hz), although the PtC coupling constant is substantially smaller. The decrease in the value of $^1J(PtC)$ is expected upon coordination to the opposite face of the Pt_3 cluster.[12]

The observation of a single carbonyl resonance in the terminal carbonyl chemical shift range for the $Ir(CO)_4$ unit suggests that it remains close to tetrahedral, but since a separate resonance with a similar chemical shift is seen for free $[Ir(CO)_4]^-$ in samples containing both **2** and excess $[Ir(CO)_4]^-$, it is clear that the $Ir(CO)_4$ unit is coordinated to the Pt_3 unit in **2** (Figure 2). The ^{31}P and ^{13}C NMR spectra remain essentially unchanged at temperatures as low as −90 °C, and so if the true structure has symmetry lower than C_3 for the $Pt_3(\mu\text{-dppm})_3$ unit or tetrahedral at iridium, there must be very easy fluxionality. We, therefore, propose that compound **2** is a weak complex between the $[Ir(CO)_4]^-$ anion and the $[Pt_3(\mu_3\text{-}CO)(\mu\text{-dppm})_3]^{2+}$ cluster cation in which the $[Ir(CO)_4]^-$ group may be protected from dissociation/exchange by the "picket-fence" of phenyl groups surrounding the coordination site. We note that the $[Pt_3(\mu_3\text{-}CO)(\mu\text{-dppm})_3]^{2+}$ cluster has previously been shown to weakly coordinate anions such as halides and

(12) (a) Jennings, M. C.; Schoettel, G.; Roy, S.; Puddephatt, R. J.; Douglas, G.; Manojlovic-Muir, Lj.; Muir, K. W. *Organometallics* **1991**, *10*, 580. (b) Lloyd, B. R.; Puddephatt, R. J. *J. Am. Chem. Soc.* **1985**, *107*, 7785.

trifluoroacetate, and the ^{31}P chemical shift of δ −22.4 in **2** shows a similar upfield shift from the free Pt_3 cluster as was observed for clusters such as $[Pt_3(\mu_3\text{-CO})(\mu_3\text{-Cl})(\mu\text{-dppm})_3]$ (δ −17.6).[13] The exact nature of the platinum−iridium bonding in **2** cannot be determined further, in the absence of a structure determination. Upon warming, compound **2** loses CO, forming compound **3**.

Rearrangement of the Butterfly Cluster 3 To Give 5. Compound **3** is stable in solution for short periods of time only. Over about 1 h it undergoes rearrangement to the isomeric compound **5**, in which the Ir now occupies a hinge position and the three dppm ligands bridge the Pt_2Ir unit, rather than the Pt_3 unit (Scheme 1). Cluster **5** is thermodynamically favored over **3** because the iridium atom now occupies a hinge position, where it can adopt an 18-electron configuration, while one of the platinum atoms that was previously in the hinge position now occupies a wingtip position and has a 16-electron count. The structure of **5** also minimizes charge separation, no longer requiring a negative charge on iridium. EHMO calculations, similar to those carried out for **3**, gave computed charges of −0.7 and +1.7 e, respectively, for the $Pt(CO)(\mu\text{-CO})_2$ and $[Pt_2Ir(\mu\text{-CO})(\mu\text{-}H_2PCH_2PH_2)_3]$ fragments.

Like **3** and **4**, cluster **5** is highly fluxional. At room temperature, the ^{31}P NMR spectrum of **5** contains three broad resonances for three nonequivalent dppm phosphorus atoms. The resonances at δ −10.4 and −17.8 show Pt satellites with typical $^1J(PtP)$ coupling constants ($^1J(PtP)$ = 3802, 3282 Hz, respectively) and are assigned to the platinum-bonded phosphorus atoms P^c and P^b (see Chart 2 for NMR atom labeling), while the third resonance at δ −18 shows no large Pt coupling and is assigned to the iridium-bound phosphorus atoms P^a. A trans P−Ir−Pt−P coupling $^3J(P^aP^c)$ = 54 Hz is observed, and a similar trans coupling through the PtPt bond between P^b and $P^{b'}$ is observed in the ^{195}Pt satellites, indicating the presence of metal−metal bonds at each edge of the Pt_2Ir triangle. The ^{31}P NMR spectrum indicates the presence of mirror symmetry bisecting the molecule through the Ir and between the two Pt atoms. At −80 °C, the symmetry is broken and the spectrum shows six broad ^{31}P resonances.

The $^{13}C\{^1H\}$ NMR spectrum of **5** contains resonances for one terminal carbonyl at $\delta(C^a)$ 191.6 that shows a large coupling $^1J(PtC)$ = 1185 Hz, indicating a terminal carbonyl on platinum, and a long-range coupling $^2J(PtC)$ = 121 Hz to two apparently equivalent platinum atoms, Pt^b and $Pt^{b'}$. Three resonances for bridging carbonyls are observed. The carbonyl on the bottom face of the $Pt_2Ir(\mu\text{-dppm})_3$ unit is observed at $\delta(C^b)$ 216 and shows no coupling to ^{195}Pt, perhaps indicating that it is bound more strongly to iridium than to platinum. The peak at $\delta(C^c)$ 218.3 is assigned as due to the carbonyl that bridges two platinum atoms, based on platinum coupling constants of $^1J(Pt^aC^a)$ = 810 Hz to a single Pt atom and $^1J(PtC)$ = 180 Hz to two apparently equivalent platinum atoms, Pt^b and $Pt^{b'}$. The carbonyl that bridges between iridium and Pt^a is observed at $\delta(C^d)$ = 235.3, with $^1J(Pt^aC^d)$ = 440 Hz.

Scheme 3

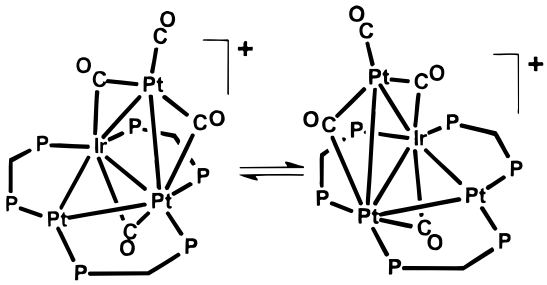

At −80 °C, the resonances due to C^b and C^d remain essentially unchanged. However, the carbonyl that bridges two platinum atoms now shows satellites with $^1J(Pt^aC^c)$ = 810 and $^1J(Pt^bC^c)$ = 360 Hz, each with intensities of 1/4, indicating coupling to a single platinum atom. The doubling of the smaller coupling constant compared to the value at room temperature is clearly due to the freezing out of a fluxional process. The ^{195}Pt satellites of the resonance due to the terminal carbonyl on Pt^a also change with temperature, but the smaller coupling is not resolved at −80 °C. The change in the ^{13}C spectrum can be explained by a fluxional process in which one side of the $Pt^a(CO)(\mu\text{-CO})_2$ unit remains anchored to the iridium atom while the other side moves between the two other platinum atoms in a windscreen-wiper fashion as shown in Scheme 3. As a result, the atom C^c is coupled to Pt^a and two equivalent Pt atoms (Pt^b and $Pt^{b'}$) at room temperature but to Pt^a and only one other platinum atom (Pt^b) when the fluxional process is frozen out; hence, the relevant coupling constant is doubled. The fluxional process occurring in **5** is subtly different than that occurring in **3**, where the $Ir(CO)(\mu\text{-CO})_2$ unit alternately bridges all three Pt−Pt bonds. In **5**, the $Pt(CO)(\mu\text{-CO})_2$ unit alternately bridges the two Pt−Ir bonds but not the Pt−Pt bond, remaining anchored at iridium. The difference between the two fluxional processes results from the unfavorable unsaturated Ir center which would be formed in cluster **5** if the $Pt(CO)(\mu\text{-CO})_2$ unit bridged the Pt−Pt bond. In other words, there is a strong preference for iridium to remain in the hinge position of the butterfly cluster where it remains coordinatively saturated both in the ground-state structure and in the transition state of the fluxional process.

The mechanism of the rearrangement of **3** to **5** is uncertain since no intermediates were detected. Since two phosphorus atoms must migrate from platinum to iridium and this is not expected to occur in a concerted fashion, it must be assumed that the second phosphorus atom migration is faster than the first.

Elimination of a Platinum Atom from Cluster 5. Cluster **5** is much more stable than **3**, but over long periods of time in solution, it loses the platinum atom that is not anchored by dppm coordination to form the trimetallic cluster $[Pt_2Ir(CO)(\mu_3\text{-CO})(\mu\text{-dppm})_3][PF_6]$, **6**. The ^{31}P NMR spectrum of **6** shows three resonances. The two at δ −2.92 (P^a) and −3.05 (P^b) have ^{195}Pt satellites with coupling constants of $^1J(PtP)$ = 3930 and 2692 Hz, respectively, while the third resonance at δ −30.84 has no large Pt coupling and is assigned to the iridium-bound phosphines (P^c). Trans coupling con-

(13) (a) Bradford, A. M. *Coordination Chemistry of a Triplatinum Cluster*; Ph.D. Thesis, The University of Western Ontario, 1989. (b) Puddephatt, R. J.; Manojlovic-Muir, Lj.; Muir, K. W. *Polyhedron* **1990**, *9*, 2767. (c) Zhang, T.; Drouin, M.; Harvey, P. D. *J. Chem. Soc., Chem. Commun.* **1996**, 877. (d) Provencher, R.; Aye, K.-T.; Drouin, M.; Gagnon, J.; Boudreault, N. *Inorg. Chem.* **1994**, *33*, 3689.

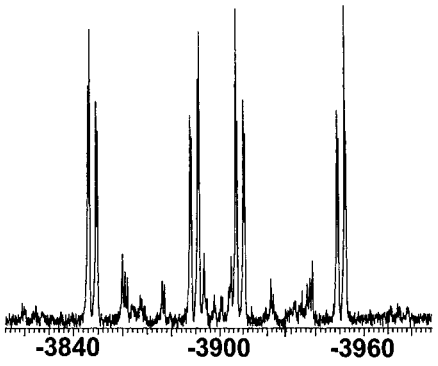

Figure 3. ^{195}Pt NMR spectrum (64.3 MHz) of $[Pt_2Ir(CO)(\mu_3\text{-}CO)(\mu\text{-}dppm)_3][PF_6]$, **6**.

Scheme 4

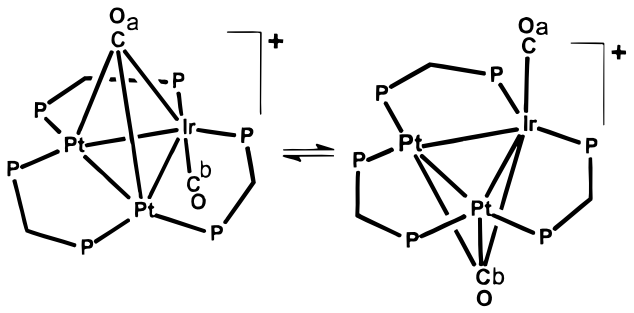

stants through metal−metal bonds $^3J(P^aP^c) = 85$ Hz and $^3J(P^bP^{b'}) = 222$ Hz are observed.

The ^{195}Pt NMR spectrum (Figure 3) confirms the proposed structure, showing one Pt resonance that appears as a doublet of doublets of doublets of doublets, resulting from couplings $^1J(PtP^a)$, $^1J(PtP^b)$, $^2J(PtP^{b'})$ and $^2J(PtP^{c'})$. Superimposed on this multiplet is a more complex one resulting from the isotopomers which contain two ^{195}Pt atoms. The ^{13}C NMR spectrum of **6** contains a sharp singlet at δ 198.9, which shows no platinum coupling, and is consistent with either a single carbonyl or two equivalent carbonyls on opposite faces of the cluster. However, the ^{1}H NMR spectrum shows only two resonances for dppm methylene groups in a 2:1 ratio, indicating that the cluster has apparent top−bottom (C_{2v}) symmetry and, therefore, must contain two carbonyls. The IR spectrum (in solution and solid state) of **6** shows two bands at 2036 and 1802 cm^{-1}, indicating the presence of one terminal and one bridging carbonyl. The observation of a single carbonyl resonance in the ^{13}C NMR spectrum indicates that, in solution, the cluster is undergoing a fast fluxional process in which the two carbonyls move between bridging and terminal coordination, rendering them equivalent (Scheme 4). This is a very facile process since the ^{13}C NMR spectrum is unchanged to −90 °C.

Cluster **6** is a heteronuclear analogue of $[Pt_3(\mu_3\text{-}CO)(\mu\text{-}dppm)_3]^{2+}$, **1**, except that it has an additional carbonyl ligand coordinated to Ir. Hence, **6** and **1** are 44- and 42-electron clusters, respectively. This reflects the greater tendency for Ir to be coordinatively saturated. Under CO pressure, cluster **1** can also coordinate a second carbonyl ligand to form $[Pt_3(\mu_3\text{-}CO)(CO)(\mu\text{-}dppm)_3]^{2+}$, **7**, which is isoelectronic and isostructural to **6** and exhibits similar spectroscopy and the same fluxional behavior as **6**.[14] Complex **7** has ν(CO) = 2075 (terminal) and 1760 (bridging) cm^{-1}.[14] Extended Hückel molecular orbital calculations on the model complex $[Pt_2Ir(CO)_2(\mu\text{-}H_2PCH_2PH_2)_3]^+$ suggest that the most favorable structure is one in which the carbonyls both occupy triply bridging positions, but there is a second minimum in which one carbonyl triply bridges and the other is in a terminal position on Ir. The spectroscopy clearly indicates that the terminal/bridging structure is the true ground-state structure and that, in this case, the level of theory is inadequate in its ability to predict the correct structure.

The rate of the conversion of **5** into **6** is increased in the presence of CO, suggesting that CO coordination is required to break the metal−metal bonds prior to elimination of the platinum. The insoluble brown side product of the reaction was not characterized.

Discussion

The overall reaction, shown in Scheme 1, is a net displacement of Pt by Ir(CO)$^-$. The initial step is coordination of the $Ir(CO)_4^-$ fragment to the $[Pt_3(\mu_3\text{-}CO)(\mu\text{-}dppm)_3]^{2+}$ cluster cation. This is followed by loss of CO to form the first butterfly cluster **3**, which has the Ir atom in a wingtip position and retains the $Pt_3(\mu\text{-}dppm)_3$ unit. This cluster is unstable relative to a more favorable arrangement with the iridium in a hinge position, and rearrangement occurs to the isomeric cluster **5**, which now contains a $Pt_2Ir(\mu\text{-}dppm)_3$ unit, with one of the Pt−Ir bonds bridged by a $Pt(CO)(\mu\text{-}CO)_2$ fragment. The final step is the elimination of Pt from **5** to form the final Pt_2Ir trimer **6**. Overall then, this provides a well-defined example of metal for metal substitution in a coordinatively unsaturated cluster complex,[5−7] in which a neutral platinum fragment is displaced by an anionic iridium fragment. Clusters **3** and **4** are particularly unusual because they contain a coordinatively unsaturated iridium center. The platinum/iridium clusters described are of considerable interest as models for Pt/Ir catalysts. One interpretation of the enhanced selectivity of Pt/Ir catalysts is that surface iridium atoms tend to be saturated and so act to dilute the active surface platinum ensembles,[2] and the increased tendency of iridium compared to platinum to be coordinatively saturated is clearly demonstrated by the chemistry described above.

Experimental Section

Infared spectra were recorded as Nujol mulls on a Perkin-Elmer 2000 FTIR spectrometer. The ^{1}H, ^{31}P{^{1}H}, and ^{13}C{^{1}H} NMR spectra were recorded on a Varian Gemini 300 NMR spectrometer, while ^{195}Pt NMR spectra were recorded on a Varian XL-300 NMR spectrometer and referenced relative to aqueous $K_2[PtCl_4]$. The cluster $[Pt_3(\mu_3\text{-}CO)(dppm)_3][PF_6]$ (**1**)[15] and $[PPN][Ir(CO)_4]$[16] were prepared according to literature methods. All manipulations were carried out using standard Schlenk techniques under an atmosphere of prepurified argon or in a Braun MB-150-M glovebox.

$[Pt_3\{Ir(CO)(\mu\text{-}CO)_2\}(\mu\text{-}CO)(\mu\text{-}dppm)_3][PF_6]$, 3. A mixture of $[Pt_3(\mu_3\text{-}CO)(\mu\text{-}dppm)_3][PF_6]_2$ (**1**, 24 mg, 0.012 mmol) and $[PPN][Ir(CO)_4]$ (10 mg, 0.012 mmol) was dissolved in CD_2Cl_2

(14) Lloyd, B. R.; Bradford, A.; Puddephatt, R. J. *Organometallics* **1987**, *6*, 424.
(15) Ferguson, G.; Lloyd, B. R.; Puddephatt, R. J. *Organometallics* **1986**, *5*, 344.
(16) Garlaschelli, L.; Della Pergola, R.; Martinengo, S. *Inorg. Synth.* **1989**, *28*, 211.

(0.5 mL). Vigorous evolution of gas (CO) occurred, and a deep red solution of $[Pt_3Ir(CO)(\mu\text{-}CO)_3(\mu\text{-dppm})_3][PF_6]$, **3**, was formed. The ^{31}P and ^{13}C NMR spectra were recorded immediately. IR: ν(CO) 1982 (m), terminal CO cm^{-1}; 1890 (s), 1807 (m), 1765 (m), bridging CO, cm^{-1}. ^{13}C NMR (CD_2Cl_2 of ^{13}CO-labeled sample): δ 188.8 (m, ^2J(PtC) = 43 Hz, terminal Ir*C*^{a}O), 214.8 (m, ^1J(PtC) = 310 Hz, $Pt_2(\mu\text{-}C^bO)$), 239.7 (s, PtIr(μ-*C*^{c}O)). ^{31}P NMR (CD_2Cl_2): −20 °C $\delta(^{31}P)$ −12.49 (s, ^1J(PtP) = 3132 Hz, ^2J(PtP) = 134 Hz, Pt*P*); at −80 °C, the resonance split into three very broad resonances centered at $\delta(^{31}P)$ −1.5, −11.5, and −21.5. Solutions of **3** are stable at room temperature only for brief periods, completely transforming into compound **5** in approximately 1 h, but are indefinitely stable at −80 °C.

$[Pt_3\{Ir(P(OPh)_3)(\mu\text{-}CO)_2\}(\mu\text{-}CO)(\mu\text{-dppm})_3][PF_6]$, 4. A mixture of $[Pt_3(\mu_3\text{-}CO)(dppm)_3][PF_6]_2$ (**1**, 26 mg, 0.013 mmol) and [PPN][Ir(CO)$_4$] (11 mg, 0.013 mmol) was dissolved in CH_2Cl_2 (1 mL), giving a deep red solution which was allowed to stir for 5 min, after which $P(OPh)_3$ (0.0039 g, 3.3 μL, 0.013 mmol) was added. The solution was stirred for a further 10 min, and then the solvent was removed in vacuo, giving a dark orange-brown residue, which was redissolved CH_2Cl_2 (1 mL). Pentane (5 mL) was then added until the solution was turbid. The solution was then cooled to 0 °C for 2 h, resulting in the formation microcrystalline solid. The orange supernatant was discarded, and the solid was dried in vacuo. Yield: 24 mg, 77%. Anal. Calcd for $C_{96}H_{81}F_6IrO_6P_8Pt_3$: C, 46.7; H, 3.3. Found: C, 46.4; H, 3.1. IR (Nujol): ν(CO) 1885 (s), 1807 (m), 1765 (m), bridging CO, cm^{-1}. ^{31}P NMR (CD_2Cl_2): $\delta(^{31}P)$ = −12.4 (m, ^1J(PtP) = 3242 Hz, ^2J(PtP) = 158 Hz, ^3J(PP) = 182 Hz, ^3J(PP) = 16 Hz, dppm Pt*P*), 121.9 (m, 1:4:7:4:1 quintet of septets, ^2J(PtP) = 508 Hz, ^3J(PP) = 16 Hz, *P*(OPh)$_3$). At −90 °C, the ^{31}P resonance of dppm split into three broad resonances at δ −7, −9, and −19.

$[Pt_3(\mu_3\text{-}CO)(\mu\text{-dppm})_3\{Ir(CO)_4\}][PF_6]$, 2. A mixture of $[Pt_3(\mu_3\text{-}CO)(dppm)_3][PF_6]_2$ (40 mg, 0.019 mmol) and [PPN][Ir(CO)$_4$] (16 mg, 0.019 mmol) was cooled to −80 °C, and CD_2Cl_2 (0.5 mL), precooled to −80 °C, was added to form a dark red solution. The ^{31}P and ^{13}C NMR, recorded at −80 °C without warming the sample, showed compound **2** as the predominant product. ^{13}C NMR (CD_2Cl_2, −80 °C): $\delta(^{13}C)$ 183.7 (s, Ir*C*O), 199.5 (m, ^1J(PtC) = 503 Hz), ^{31}P NMR $\delta(^{31}P)$ −22.43 (s, ^1J(PtP) = 3415 Hz, ^2J(PtP) = 220 Hz, Pt*P*). On warming, resonances due to **3** grew in and those due to **2** decayed. Charging the tube with CO led to an increase in the abundance of **2** with respect to **3**.

$[Pt_2Ir\{Pt(CO)(\mu\text{-}CO)_2\}(\mu\text{-}CO)(\mu\text{-dppm})_3][PF_6]$, 5. A solution of **3** was prepared as above from $[Pt_3(\mu_3\text{-}CO)(\mu\text{-dppm})_3][PF_6]_2$ (200 mg, 0.097 mmol) and [PPN][Ir(CO)$_4$] (82 mg, 0.097 mmol) in CH_2Cl_2 (30 mL). The solution was stirred for 1 h, the solvent was removed in vacuo, and the red-orange residue was extracted into THF and filtered. The volume of solvent was reduced to 3 mL, and **5**, as a bright orange powder, was precipitated by slow addition of Et_2O, then separated and washed with Et_2O (3 × 10 mL) and dried in vacuo. Yield: 173 mg, 81%. The complex typically contained about 5% impurity of either **3** or **6**, as analyzed by NMR, and so good analytical data were not obtained. IR(Nujol): ν(CO) 1987 (sb, (terminal CO), 1808 (s), 1769 (s), bridging CO, cm^{-1}. ^{13}C NMR (CD_2Cl_2): $\delta(^{13}C)$ 191.6 (m, ^1J(PtC) = 1185 Hz, ^2J(PtC) = 121 Hz, Pt*C*^{a}O), 216 (s, $IrPt_2(\mu\text{-}C^bO)$), 218.3 (m, ^1J(PtC) = 810, 180 Hz, $Pt_2(\mu\text{-}C^cO)$), 235.3 (m, ^1J(PtC) = 440 Hz, PtIr(μ-C^{d}O)). ^{31}P NMR $\delta(^{31}P)$ −10.4 (m, ^3J(PP) = 54 Hz, ^1J(PtP) = 3802 Hz, Pt*P*^{c}), −17.8 (m, ^1J(PtP) = 3282 Hz, Pt*P*^{b}), −18 (m,^3J(PP) = 54 Hz, Ir*P*^{a}). At −80 °C, $\delta(^{13}C)$ 191.2 (m, ^1J(PtC) = 1200 Hz, ^2J(PtC) not resolved, Pt*C*^{a}O), 215.8 (s, $IrPt_2(\mu\text{-}C^bO)$), 218.8 (m, ^1J(PtC) = 810 Hz, 360 Hz, $Pt_2(\mu\text{-}C^cO)$), 235.3 (m, ^1J(PtC) = 440 Hz, PtIr(μ-C^{d}O)); $\delta(^{31}P)$ = −2, −4, −11, −12, −19, −21 (br m, dppm).

$[Pt_2Ir(CO)(\mu_3\text{-}CO)(\mu\text{-dppm})_3][PF_6]\cdot 2CH_2Cl_2$, 6. A sample of **3** was prepared as above from $[Pt_3(\mu_3\text{-}CO)(dppm)_3][PF_6]$ (29 mg, 0.014 mmol) and [PPN][Ir(CO)$_4$] (12 mg, 0.014 mmol), and the resulting solution was stirred under CO (1.4 atm) for 7 days, resulting in a gradual color change from deep red to dark brown. At this point, cluster **6** was the only phosphorus-containing species as shown by ^{31}P NMR. The solvent was removed in vacuo, the residue was passed through a column of alumina using CH_2Cl_2/pentane (90/10) as the eluant, and a bright orange band was isolated. Yield: 10 mg, 36%. ^1H NMR: δ 5.72 (m, 2H, dppm CH_2), 5.35 (m, 4H, dppm CH_2). Bright orange crystals of **6**·$2CH_2Cl_2$ were grown by slow diffusion of Et_2O into a CH_2Cl_2 solution. Anal. Calcd for $C_{79}H_{70}Cl_4F_6IrO_2P_7Pt_2$: C, 45.0; H, 3.3. Found: C, 44.8; H, 3.4. IR(Nujol): ν(CO) 2036 (s), terminal CO), 1802 (s), bridging CO) cm^{-1}. ^{13}C NMR (CD_2Cl_2): $\delta(^{13}C)$ 198.9 (s, *C*O). ^{31}P NMR $\delta(^{31}P)$ −2.92 (m, ^1J(PtP) = 3930 Hz, ^2J(PtP) = 34 Hz, $^2J(P^aP^b)$ = 3 Hz, $^2J(P^aP^{a'})$ = 27 Hz, $^3J(P^aP^c)$ = 85 Hz, PtP^a), −3.05 (m, ^1J(PtP) = 2692 Hz, ^2J(PtP) = 211 Hz, $^2J(P^aP^b)$ = 3 Hz, $^3J(P^bP^{b'})$ = 222 Hz, Pt^b), −30.84 (m, ^2J(PtP) = 8 Hz, $^3J(P^aP^c)$ = 85 Hz, IrP^c).

Extended Huckel Molecular Orbital Calculations. Calculations were carried out on the model complexes $[Pt_3\{Ir(CO)(\mu\text{-}CO)_2\}(CO)(\mu\text{-}H_2PCH_2PH_2)_3]^+$ and $[Pt_2Ir\{Pt(CO)(\mu\text{-}CO)_2\}(CO)(\mu\text{-}H_2PCH_2PH_2)_3]^+$ by using the program CACAO.[17] Idealized structures based on mean bond parameters from the structure of **4** and the standard parameters supplied with the program were used. Calculations were also carried out for the complex $[Pt_2Ir(CO)_2(\mu\text{-}H_2PCH_2PH_2)_3]^+$ with the carbonyl positions in both the triply bridging position and the terminal position on Ir and at intermediate positions. In these calculations, the shorter IrC distance was maintained at a constant value and the carbonyl was held perpendicular to the Pt_2Ir plane.

X-ray Structure Determination. Data were collected using a Siemens P4 diffractometer fitted with a CCD detector. The crystal data and refinement parameters are summarized in Table 2. The space group was determined from systematic absences. A semiempirical absorption correction was applied. The structure was solved using direct methods, completed by subsequent Fourier syntheses, and refined using full-matrix, least-squares methods.[18]

Acknowledgment. We thank the NSERC (Canada) for financial support.

Supporting Information Available: Tables of X-ray data for complex **4** (14 pages). Ordering information is given on any current masthead page.

OM9800952

(17) Mealli, C.; Proserpio D. M. *J. Chem. Educ.* **1990**, 67, 399.
(18) Sheldrick, G. M. University of Göttingen, Göttingen, Germany, 1993.